

Investigation of $\pi^-p \rightarrow K_1^0 K_1^0 n$ at 4 and 5 GeV/cT. F. HOANG, D. P. EARTLY,* J. J. PHELAN,† A. ROBERTS,‡ AND C. L. SANDLER§
Argonne National Laboratory,|| Argonne, Illinois 60439

AND

S. BERNSTEIN, S. MARGULIES, AND D. W. MCLEOD
University of Illinois at Chicago Circle, Chicago, Illinois 60680

AND

T. H. GROVES,¶ N. N. BISWAS, N. M. CASON, V. P. KENNEY, J. M. MARRAFFINO,**
J. T. MCGAHAN, J. A. POIRIER, AND W. D. SHEPHARD

Department of Physics, University of Notre Dame,†† Notre Dame, Indiana 46556

(Received 28 April 1969)

The reaction $\pi^-p \rightarrow K_1^0 K_1^0 n$ has been investigated at 4 and 5 GeV/c in a spark-chamber experiment. The threshold enhancement in the s -wave $K_1^0 K_1^0$ system is observed and can be fitted either by a complex scattering length or by a resonance form. An enhancement is also evident in the region of the f^0 and A_2^0 mesons, but no unambiguous interpretation of this effect can be given.

I. INTRODUCTION

IN an attempt to improve our understanding of the $K_1^0 K_1^0$ system,¹⁻⁶ we have investigated the reaction $\pi^-p \rightarrow K_1^0 K_1^0 n$ at 4 and 5 GeV/c in a spark-chamber experiment performed at the Zero Gradient Synchrotron at Argonne National Laboratory. A preliminary report of our results has been published elsewhere.⁷

The K_1^0 -pair invariant-mass spectrum exhibits a prominent $I=0$, $J^P=0^+$ enhancement just above threshold, as well as additional structure at higher masses. The threshold enhancement has been alter-

nately interpreted as resulting from an isoscalar s -wave $K^0 \bar{K}^0$ interaction²⁻⁴ or from an $I=0$, $J^P=0^+$ resonant state,^{5,6} while the structure at higher masses has been taken to be indicative of the $K_1^0 K_1^0$ decay modes of the $f^0(1250)$ and $A_2^0(1300)$ mesons (and perhaps others).

The first discussion of the K_1^0 -pair final state produced in π^-p interactions was given by Erwin *et al.*,¹ who attempted to estimate the $\pi\pi \rightarrow K\bar{K}$ cross section by applying the Chew-Low one-pion exchange (OPE) model⁸ to a total of 19 events obtained in $\pi^-p \rightarrow K_1^0 K_1^0 n$ at 1.89 and 2.10 GeV/c. A more quantitative study was performed by Alexander *et al.*,² using a sample of 66 events obtained at momenta between 1.5 and 2.3 GeV/c. In addition to finding evidence of $Y_0^*(1520)$ production in the $K_1^0 n$ system, a sharply peaked enhancement was observed near threshold in the $K_1^0 K_1^0$ final state but not in the $K_1^0 K^-$ final state, implying an $I=0$ effect.⁹ The K_1^0 -pair production was found to be peripheral and indicative of OPE. The threshold enhancement was attributed to a strong $I=0$, $J^P=0^+$ interaction in the $K\bar{K}$ system, and the Chew-Low approach was employed to analyze the $\pi\pi \rightarrow K\bar{K}$ vertex. Further support for this interpretation was presented by Hess *et al.*³ and Dahl *et al.*⁴ (working in conjunction). In a systematic study of strange-particle production in π^-p interactions, these authors obtained a total of 426 $K_1^0 K_1^0 n$ events at beam momenta between 1.6 and 4.2 GeV/c. Following the analysis of Alexander *et al.*,² they described the threshold enhancement in terms of a zero-effective-range, complex-scattering-length parametrization of the $K\bar{K}$ system.

⁸ G. F. Chew and F. E. Low, Phys. Rev. **113**, 1640 (1958).

⁹ Threshold enhancements in the $K^0 K^\pm$ system implying an $I=1$ effect have been reported in $p\bar{p}$ annihilations by R. Armenteros, D. Edwards, T. Jacobsen, L. Montanet, J. Vandermeulen, Ch. D'Andlau, A. Astier, P. Baillon, J. Cohen-Ganouna, C. Defoix, J. Slaud, and P. Rivet [Phys. Letters **17**, 344 (1965)], and by C. Baltay, J. Lach, J. Sandweiss, H. D. Taft, N. Yeh, D. L. Stonehill, and R. Stump [Phys. Rev. **142**, 932 (1966)]. No such peaks are reported in Refs. 2-5, where π^-p interactions are studied.

* Associated Midwestern Universities Predoctoral Research Fellow.

† Based in part on the dissertation of JJP submitted to Saint Louis University in partial fulfillment of requirements for the Ph.D. degree. Present address: Rutherford High Energy Laboratory, Chilton, Didcot, Berkshire, England.

‡ Present address: National Accelerator Laboratory, Batavia, Ill.

§ Present address: Academy for Interscience Methodology, Chicago, Ill.

|| Work supported by the U. S. Atomic Energy Commission.

¶ Present address: Argonne National Laboratory, Argonne, Ill.

** Based in part upon the dissertation of JMM submitted to the University of Notre Dame in partial fulfillment of requirements for the Ph.D. degree. Present address: University of California at San Diego, LaJolla, Calif.

†† Work supported in part by the National Science Foundation.

¹ A. R. Erwin, G. A. Hoyer, R. H. March, W. D. Walker, and T. P. Wangler, Phys. Rev. Letters **9**, 34 (1962).

² G. Alexander, O. I. Dahl, L. Jacobs, G. Kalbfleisch, D. H. Miller, A. Rittenberg, J. Schwartz, and G. A. Smith, Phys. Rev. Letters **9**, 460 (1962).

³ R. I. Hess, O. I. Dahl, L. M. Hardy, J. Kirz, and D. H. Miller, Phys. Rev. Letters **17**, 1109 (1966).

⁴ O. I. Dahl, L. M. Hardy, R. I. Hess, J. Kirz, and D. H. Miller, Phys. Rev. **163**, 1377 (1967).

⁵ D. J. Crennell, G. R. Kalbfleisch, K. W. Lai, J. M. Scarr, T. G. Schumann, I. O. Skillicorn, and M. S. Webster, Phys. Rev. Letters **16**, 1025 (1966).

⁶ W. Beusch, W. E. Fischer, B. Gobbi, M. Pepin, E. Polgar, P. Astbury, G. Brautti, G. Finochiaro, J. C. Lassalle, A. Michelini, K. M. Terwillinger, D. Websdale, and C. H. West, Phys. Letters **25B**, 357 (1967).

⁷ T. F. Hoang, D. P. Eartly, J. J. Phelan, A. Roberts, C. L. Sandler, S. Bernstein, S. Margulies, D. W. McLeod, T. H. Groves, N. N. Biswas, N. M. Cason, V. P. Kenney, J. M. Marraffino, J. T. McGahan, J. A. Poirier, and W. D. Shephard, Phys. Rev. Letters **21**, 316 (1968).

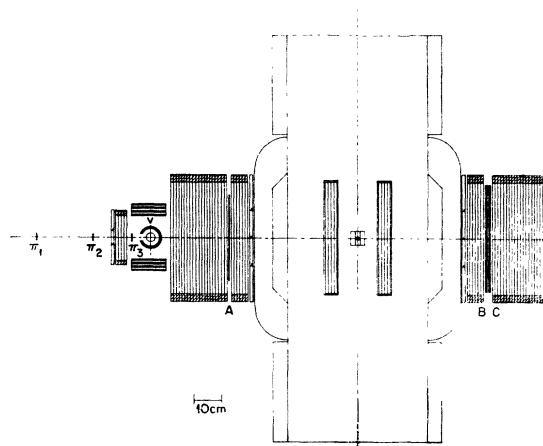


FIG. 1. Plan view of the apparatus.

The real part of the scattering length was found to be between about 2 and 10 F.

A different interpretation of the threshold enhancement was proposed by Crennell *et al.*,⁵ who investigated $\pi^\pm p$ interactions at 6 GeV/c. Their data, consisting of 178 $K_1^0 K_1^0 n$ events and 206 $K_1^0 K_1^0 +$ neutrals events, exhibit a narrow peak above the $K_1^0 K_1^0$ threshold. This was interpreted as an $I=0, J^P=0^+$ resonant state, the S^* , with a mass $M_0=1.068\pm 0.010$ GeV/c² and a width $\Gamma_0=0.080\pm 0.015$ GeV/c². In addition, the structure evident in their data at higher invariant masses appears to include not only contributions from the $K_1^0 K_1^0$ decay modes of the f^0 and A_2^0 , as observed in other experiments, but also from the $f^*(\sim 1500)$. Furthermore, no $Y_0^*(1520)$ production was noted. The S^* interpretation was also favored by Beusch *et al.*,⁶ who based their findings on 2559 $K_1^0 K_1^0 n$ events obtained in a spark-chamber experiment performed at 5, 7, and 12 GeV/c. A resonance fit to the combined data in the threshold region yielded the parameters $M_0=1.079_{-0.005}^{+0.006}$ GeV/c², $\Gamma_0=0.168_{-0.019}^{+0.021}$ GeV/c², the width differing considerably from that reported by Crennell *et al.*⁵ At higher masses, Beusch *et al.*⁶ observed the $K_1^0 K_1^0$ decay of the f^0 and A_2^0 , as well as a peak at 1.435 GeV/c² which they attributed to a zero-strangeness, even-spin, positive-parity meson, the $G(\sim 1440)$. No $Y_0^*(1520)$ production was observed.

The results described above fall into two classes: Experiments performed at low momenta (below about 4 GeV/c) suggest (a) that the $K_1^0 K_1^0$ threshold enhancement is due to an interaction in the isoscalar s -wave $K\bar{K}$ system which can be described in terms of a complex scattering length, (b) that the structure at higher masses probably results from the $K_1^0 K_1^0$ decay mode of only the f^0 and A_2^0 mesons, and (c) that there is some $Y_0^*(1520)$ production in the $K^0 n$ system. On the other hand, experiments at higher momenta (5 GeV/c and above) suggest (a) that the threshold enhancement is due to an $I=0, J^P=0^+$ resonant state, (b) that higher-mass mesons are produced in addition

to the f^0 and A_2^0 , and (c) that there appears to be no $Y_0^*(1520)$ production. In an attempt to bridge these two regions, we have investigated the reaction $\pi^- p \rightarrow K_1^0 K_1^0 n$ at 4 and 5 GeV/c incident pion momentum.

II. EXPERIMENTAL DETAILS

Our experiment was performed at the zero gradient synchrotron (ZGS) at Argonne National Laboratory. The equipment, consisting essentially of a magnet-spark-chamber spectrometer and a liquid-hydrogen target, is shown in Fig. 1.

A high-momentum π^- beam, produced at about 4° from an internal Be target, was brought to about a $\frac{3}{4}$ -in.-diam focus at the liquid-hydrogen target. The beam had a momentum bite of $\pm \frac{3}{4}\%$, and the intensity was typically 30×10^8 π^- 's spread over a 200-msec spill time, with a repetition rate of 25 pulses/min. The hydrogen target consisted of a vertical cylinder of 10-mil-thick H film,¹⁰ 2 in. in diameter and 3 in. high, with brass end caps. The surrounding vacuum jacket was a concentric 3-in.-o.d., $\frac{1}{4}$ -in.-thick cylinder of Pilot-B scintillator,¹¹ having a $1\frac{1}{4}$ -in.-diam hole covered with a 10-mil H-film window for the incident beam. The vacuum jacket also served as an anticoincidence counter (V) with a measured efficiency of 99.997%.

Two lead-scintillator sandwich counters, subtending about $\frac{1}{4}$ of the total solid angle, were located on either side of the target and served to detect photons. These counters were not used in the triggering logic, but flashed signal lights which were recorded on the event photographs.

The magnet-spark-chamber spectrometer has been described in detail elsewhere.¹² The analyzing magnet has an aperture 30 cm high \times 74 cm wide \times 50 cm deep. Two slots, 40 cm long \times 5 cm wide and 30 cm long \times 5 cm wide, cut into the top and one side of the yoke, respectively, serve for viewing internally placed spark chambers. The magnetic field was set for about 10 kG at the center of the magnet. All spark chambers were constructed of 1-mil-thick aluminum foil epoxied to Lucite frames, and had 1-cm-wide gaps. The positions of incoming pions in a plane normal to the beam were determined by a 6-in.-square, four-gap beam chamber located directly upstream from the target. Charged secondaries from K_1^0 (or Λ) decay were detected in the "upstream chamber," an array of 26 gaps placed upstream from the magnet, each with an effective area 30 cm high \times 40 cm wide. A similar "downstream chamber" was placed directly behind the magnet. Two 30-cm-high \times 40-cm-wide "upstream/downstream slot chambers" were located within the magnet aperture to aid in following decay secondaries through the spectrometer.

¹⁰ Kapton, type H, E. I. Dupont de Nemours & Co., Wilmington, Del.

¹¹ Pilot Chemicals, Inc., Watertown, Mass.

¹² T. F. Hoang, G. L. Niemeier, J. J. Phelan, and T. H. Groves, *Rev. Sci. Instr.* **38**, 861 (1967).

All spark chambers were viewed from the top and side using a 90°-stereo optical system. The upstream top, upstream side, downstream top, and downstream side views were each observed through a 47-cm-high \times 64-cm-wide Lucite spherical field lens of 3.05-m focal length, and the four views were folded onto a $\frac{3}{4}$ -in. \times 1-in. (double 35-mm) frame by a mirror system. The total demagnification of the system was 74 to 1. The camera was a Flight Research¹³ model 4C fitted with a 4.5-cm focal-length lens, and had a 50-msec advance time.

Event selection (triggering) was determined by six scintillation counters positioned as shown in Fig. 1. All counters were made of Pilot-B scintillator.¹¹ The incident pion beam was defined by counters π_1 , π_2 , and π_3 , each a 1-in.-diam \times $\frac{1}{8}$ -in.-thick circular disk. As described above, the target vacuum jacket also served as an anticoincidence counter V to restrict triggering to neutral final states. Counter A, 23.0 cm high \times 30.5 cm wide \times 3 mm thick, was located after the 20th gap of the upstream chamber and served to ensure that a vertex from the charged decay of at least one of the neutrals was visible in the upstream chamber. Counter C, 27.2 cm high \times 38.0 cm wide \times 6 mm thick, located downstream from the magnet, ensured that at least one charged secondary passed through the spectrometer. Counters A and C were positioned symmetrically with respect to the center of the magnet. Counter B, a hodoscope of four horizontal counters of total area equal to C, was adjacent to C and was intended to restrict triggering to two or more emerging secondaries. However, Monte Carlo calculations indicated that such a triggering requirement would greatly reduce the event rate and would introduce an additional bias. Since a single momentum-analyzed secondary does provide sufficient kinematic information to overdetermine the hypothesis $\pi^- p \rightarrow K_1^0 K_1^0 n$, the output of B was not included in the trigger but served instead to flash signal lights which were recorded on the event photographs.

The electronics employed in this experiment consisted of standard fast-logic modules. The event trigger required to pulse the spark chambers was $\pi_1 \pi_2 \pi_3 \bar{V} AC$. After the occurrence of an event trigger, the electronics were gated off for an interval of about 65 msec to allow the system to recover. The average event rate was somewhat greater than one trigger per ZGS pulse. At the completion of the run, the data consisted of about 240×10^3 pictures at 4 GeV/c incident pion momentum, about 200×10^3 pictures at 5 GeV/c, and about 7×10^3 pictures from a background run at 4 GeV/c with the hydrogen target empty.

III. DATA ANALYSIS

The analysis of the data was carried out concurrently at Argonne National Laboratory (ANL), the Uni-

¹³ Flight Research, Inc., subsidiary of the Giannini Scientific Corp., Richmond, Va.

versity of Illinois at Chicago Circle (UICC), and at the University of Notre Dame (ND). The scanning of the film was performed at all three of these laboratories; event measuring and the spatial reconstruction computations were performed by the ANL and UICC groups at Argonne, and by the ND group at Notre Dame. Kinematic fitting and summarization were performed in common, for the most part.

A. Film Processing

Since identification of double- V events and the subsequent pairing of corresponding tracks proved to be quite difficult because of the 90°-stereo optical system employed, scanning was carried out in two stages. The first-stage criteria were (1) that a possible double- V event appear in both views of the upstream chamber, (2) that both V 's point back approximately to the target location, and (3) that at least one of the tracks be visible in a slot chamber and pass through the spectrometer magnet into the downstream chamber. Most of the film was scanned twice, subject to these criteria. The total yield of possible double- V events was about 4%, and the efficiency for finding measurable events was estimated to be 80–90% for most of the film.¹⁴

A second-stage scan, designated as an "edit," followed. Measurement candidates were selected by requiring that the event exhibit a clear double- V topology with unambiguously paired tracks in all views, that at least one prong be measurable for momentum determination, and that the beam chamber exhibit a valid beam track. Events that satisfied these criteria were sketched on an edit sheet, with the V 's identified and corresponding tracks labeled to facilitate measurement.

After the second scanning stage the data sample consisted of 4006 and 4961 candidates at 4 and 5 GeV/c, respectively. These events were then measured on image-plane digitizers. Primarily because of the difficulty in identifying and interpreting double- V events, a generous remeasurement policy was adopted, with the result that after computer processing of the measurements about $\frac{1}{2}$ of the data were remeasured after being reedited.

B. Event Identification

The first step in the processing of the measurements was the spatial reconstruction of the events and the determination of the momentum of tracks passing through the spectrometer. All tracks that were visible in at least one slot chamber and which had upstream

¹⁴ The 4-GeV/c data include a group of 206 events (from about $\frac{1}{3}$ of the 4-GeV/c film) for which the efficiency for obtaining events is about 0.7 of that for the remaining 727 events. The $K_1^0 K_1^0$ mass distribution for these 206 events differs somewhat in appearance from that for the 727 events, exhibiting less of an enhancement near threshold. Since a test of the null hypothesis for the difference distribution gave a χ^2 of 27.3 for 26 degrees of freedom, the smaller sample was added to the larger one. The results presented change by less than 1 standard deviation if the 206 events are excluded.

TABLE I. Results from the kinematical fitting of an event having four tracks with momentum determinations. It is apparent that reducing the amount of momentum information did not significantly affect the results.

Momenta (MeV/c)	p_1	p_2	p_3	p_4	$K_1^0 K_1^0$ mass (MeV/c ²)	Missing mass (MeV/c ²)
	Measured value, with error					
	591±32	1365±95	723±44	1319±114
	Fit results for specified input momenta					
p_1, p_2, p_3, p_4	573±23	1295±61	728±24	1348±69	1009.7±3	928.7±40
p_1, p_3	593	1250	713	1386	1009.3	943.7
p_2, p_4	538	1329	729	1346	1010.6	925.4
p_1	593	1250	690	1408	1009.2	945.1
p_2	539	1326	692	1385	1009.8	915.9
p_3	604	1236	713	1389	1009.2	947.3
p_4	602	1242	729	1368	1009.2	957.5

and downstream segments at least four gaps long were considered suitable for momentum analysis. Dip and azimuthal angles were determined for all upstream tracks at least four gaps long. The momentum determination was checked by measuring beam tracks from pictures taken with the hydrogen target removed. The results indicated a precision of about 5% for 1.5-GeV/c tracks. The reconstruction precision was about 1 mm in real space.

In order to investigate the spatial origin of double- V events, the distribution of the computed position of the production vertex (along the beam direction) was obtained for a sample of 744 events at 4 GeV/c. The distribution is shown in Fig. 2. As can be seen, the production point falls predominantly within the confines of the target, production from the walls and outside the target being negligible. The peaking of the distribution at the downstream end of the target is due to the increased decay probability (and, consequently, veto probability) for events produced near the upstream end. That production was restricted to the target volume was also verified experimentally in the target-empty run, during which the event rate decreased by about a factor of 15.

The reliability of the momentum determination was examined by computing the invariant mass from K_1^0

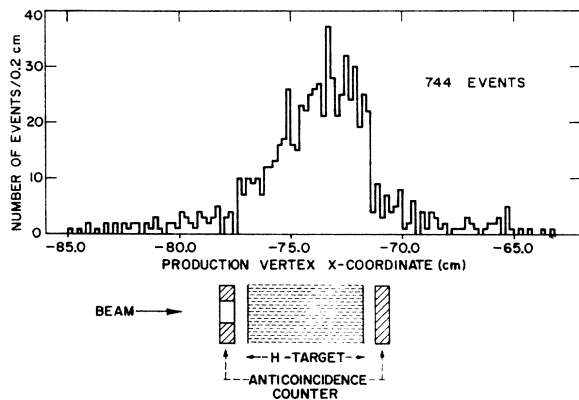


Fig. 2. Distribution of the production vertex (computed) along the beam direction for a sample of the 4-GeV/c data.

V 's, for which momentum measurements were available for both tracks. The results shown in Fig. 3 are in good agreement with the accepted value of the K_1^0 mass.

Kinematic analysis was performed using the CERN generalized least-squares program GRIND.¹⁵ The hypotheses tested were $K_1^0 K_1^0 n$, $K_1^0 \Lambda \pi^0$, $K_1^0 \Lambda$, and $K_1^0 \Sigma^0$ final states resulting from a $\pi^- p$ interaction. Each V was tested for the decay hypotheses $K_1^0 \rightarrow \pi^+ \pi^-$ and $\Lambda \rightarrow p \pi^-$, and the results of the individual V fits were used as input data for hypothesis testing at the production vertex. Data from these "single-vertex fits" were then used as input for an attempted "multivertex fit," an over-all simultaneous fit at all three vertices. Approximately $\frac{3}{4}$ of the final data had multivertex fits (four- to seven-constraint fits, depending on the number of tracks with measured momentum); the remaining $\frac{1}{4}$ had only single-vertex (one-constraint) fits.

About 80% of the $K_1^0 K_1^0 n$ events satisfied only the minimum trigger requirement of having a single decay secondary pass completely through the spectrometer. Of the remainder, about 20% had two passing secondaries, a few percent had three, and six events had all four decay products passing completely through the system. Some of the $K_1^0 K_1^0 n$ events for which momen-

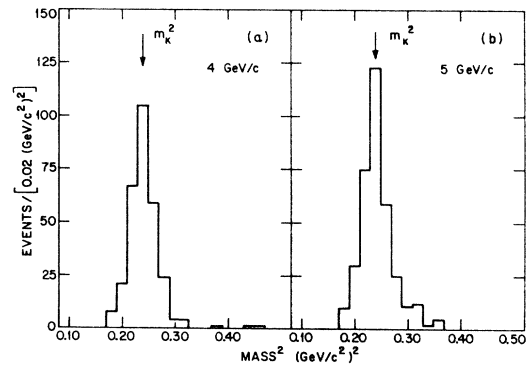


Fig. 3. Distributions of the square of the K_1^0 mass. The data shown are a subsample of all $K_1^0 V$'s having momentum determinations for both tracks.

¹⁵ R. Bock, CERN Report No. 60-30, 1960 (unpublished), and CERN Report No. 61-29, 1961 (unpublished).

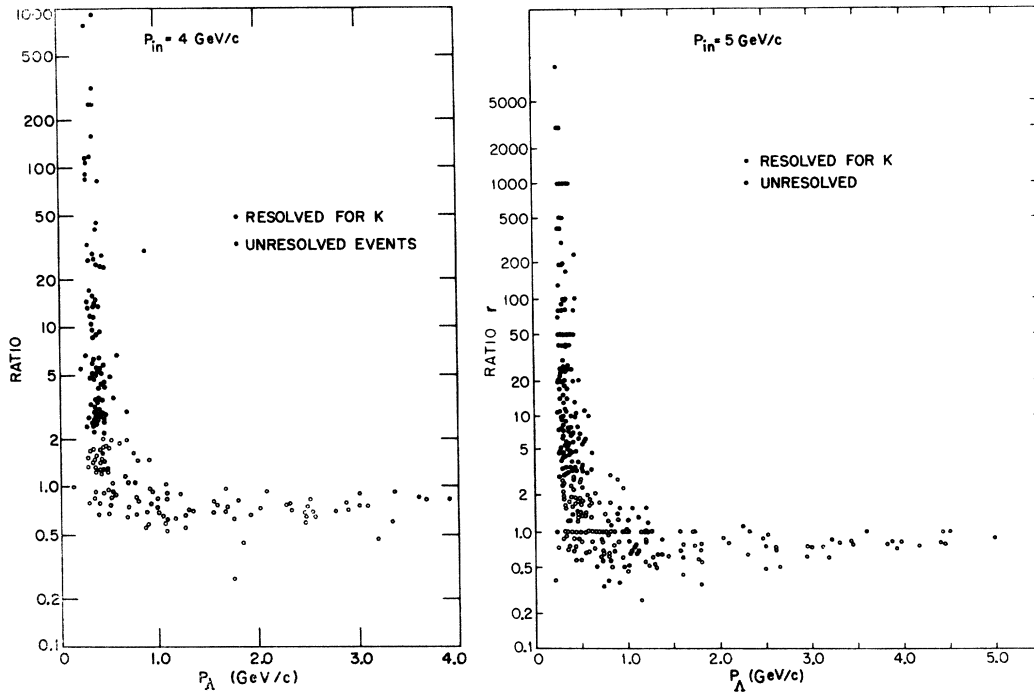


FIG. 4. Distributions of the ratio of the K_1^0 survival probability to the Λ survival probability as a function of the Λ momentum for a subsample of the data.

tum determinations were available for three or four tracks were used to test our ability to analyze less constrained events correctly. This was done by successively deleting measured momentum values (in all combinations) and processing these events through GRIND as four-, three-, two-, and one-track events. These tests indicated that neither the identification of a $K_1^0 K_1^0 n$ event nor the subsequent computation of the $K_1^0 K_1^0$ effective mass was appreciably affected by this procedure, thereby checking the validity of the one-track events. The results of this procedure for the case of one four-track event are given in Table I.

Following kinematic analysis, event information was processed using the Lawrence Radiation Laboratory (LRL) data-summary program SUMX.¹⁶ At this stage, all relevant kinematic variables, angles, and weights were computed and stored on a data-summary tape.

C. Hypothesis Ambiguities

The problem presented by events with ambiguities between the $K_1^0 K_1^0 n$ and the $K_1^0 \Lambda \pi^0$ and/or $K_1^0 \Sigma^0$ hypotheses was investigated in detail. Such ambiguities sometimes occurred when one of the individual V fits was ambiguous, a condition which generally resulted for V 's where neither track had a measured momentum. In many cases it was possible to resolve such ambiguities on the basis of a comparison of the K_1^0 and Λ

survival probabilities. For a V having no tracks with measured momentum and satisfying both the K_1^0 and Λ hypotheses, the momentum of the neutral is computed only from the decay opening angle; thus, the momenta p_K and p_Λ corresponding to these two possibilities are not independent, but are related through the decay kinematics. As a consequence, the ratio of the K_1^0 survival probability to the Λ survival probability, $r = \exp(-M_K L / p_K c \tau_K) / \exp(-M_\Lambda L / p_\Lambda c \tau_\Lambda)$, is really a function of only one of the two momenta, say, p_Λ . In this expression, L is the distance traversed by the neutral, c is the velocity of light, and M_K , τ_K and M_Λ , τ_Λ are the mass and lifetime of the K_1^0 and Λ , respectively.

The distributions of r as a function of p_Λ are shown in Fig. 4. These plots indicate the existence of two distinct regions: a vertical region of large r and low p_Λ and a horizontal region of low r and large p_Λ . Since most of the slow- Λ events were vetoed by the target anticoincidence counter, it was assumed that most of the ambiguous slow- Λ fits were actually K_1^0 decays accidentally fit as Λ 's. Because of the strong correlation between p_Λ and r , this amounts to a condition on r . Thus, for an ambiguous event to be accepted (resolved) as a $K_1^0 K_1^0 n$ event, r was required to equal or exceed 2 at 4 GeV/c, and 3 at 5 GeV/c. About 40% of the final $K_1^0 K_1^0 n$ sample consists of events selected in this way, although the fraction decreases to 25% when only the important threshold region is considered.

The effect of this selection procedure can be seen

¹⁶ Lynn Champomier, University of California Radiation Laboratory Report No. UCRL-11222, 1964 (unpublished).

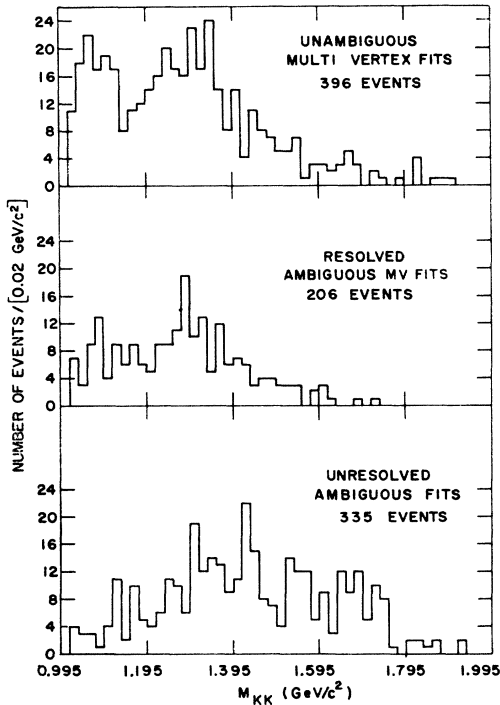


FIG. 5. Distributions of the $K_1^0 K_1^0$ invariant mass for three classes of events from the 4-GeV/c data.

from Fig. 5, where the calculated $K_1^0 K_1^0$ invariant-mass distributions are plotted separately for unambiguous, resolved, and unresolved events. The resolved and unambiguous distributions are consistent, while the unresolved and unambiguous distributions are not.

D. Events with Additional π^0 's

A further experimental difficulty was encountered in discriminating against $K_1^0 K_1^0 n \pi^0$ events in which the π^0 had low kinetic energy in the laboratory system. Events of this type would sometimes fit the $K_1^0 K_1^0 n$ hypothesis, particularly at 5 GeV/c. The presence of these events would be expected to distort the (neutral) missing-mass-squared distribution—nominally a Gaussian shape centered about the square of the neutron mass—so as to contain an excess of events above this value. That this is indeed the case can be seen from Fig. 6, which displays the missing-mass-squared distributions for all events fitted by GRIND to the $K_1^0 K_1^0 n$ hypothesis with a χ^2 probability greater than 1%. By fitting a Gaussian curve to the data below the neutron mass, reflecting this curve about the neutron mass, and then determining the excess events above the neutron mass (see Fig. 6), we have estimated the contamination in our sample due to $K_1^0 K_1^0 n \pi^0$ events to be about 10% at 4 GeV/c and 35% at 5 GeV/c at this stage of the analysis. These findings are consistent with present bubble-chamber results.¹⁷

¹⁷ J. Bartsch, L. Bondar, R. Speth, G. Hotop, G. Knies, F. Storim, J. M. Brownlee, N. N. Biswas, D. Luers, N. Schmitz, R. Seeliger, and G. P. Wolf, Nuovo Cimento 43, 1010 (1966).

To investigate the effects of this contamination, the $K_1^0 K_1^0$ invariant-mass distributions were compared for samples for which the missing-mass upper limit for acceptable events was successively set at 1.35, 1.23, and 0.94 (neutron mass) GeV/c². Fits to these three spectra were essentially identical, leading us to conclude that the results are insensitive to this effect. This was also the conclusion of Crennell *et al.*¹⁸

E. Final Data Selection

In order to exclude possibly misidentified events, two cuts were applied to the entire data sample. At this point, multivertex and single-vertex fits were accepted as $K_1^0 K_1^0 n$ events only if the χ^2 probability for this hypothesis was equal to or greater than 1%. (The distributions of χ^2 and χ^2 probability for the one-, four-, and five-constraint-fit methods were consistent with the expected theoretical distributions.) In addition, the unfitted neutral missing mass (i.e., the neutron mass) was required to be between 0.65 and 1.23 GeV/c². (See Fig. 6.) Although some $K_1^0 K_1^0 n \pi^0$ events were thereby included, the effects of this contamination on the results appear to be negligible, as discussed above. After these cuts, the final $K_1^0 K_1^0 n$ samples contained 933 and 1036 events at 4 and 5 GeV/c, respectively.

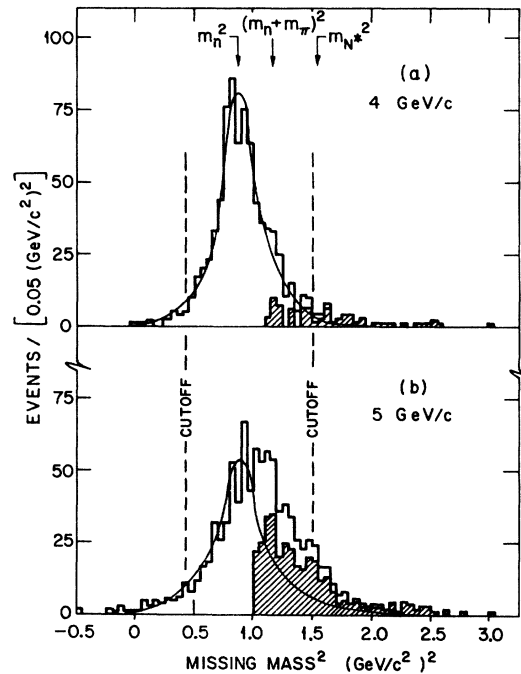
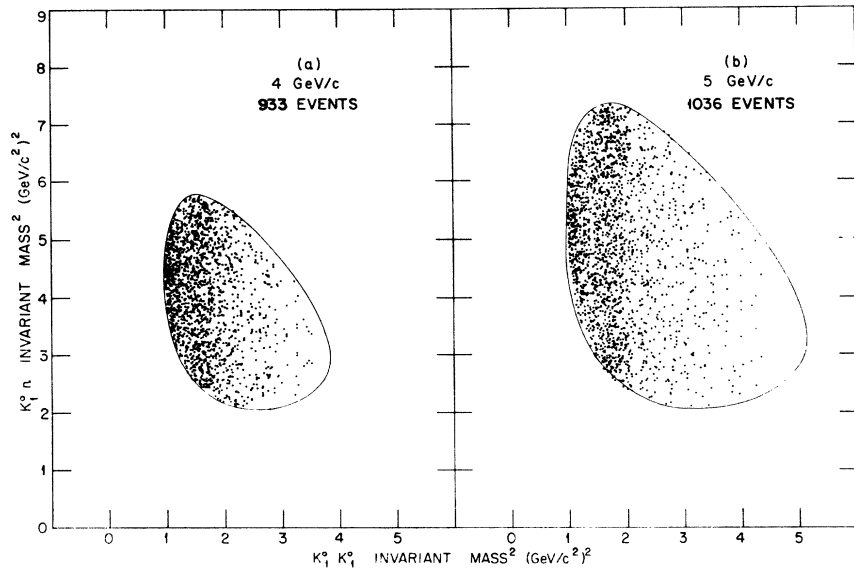


FIG. 6. Distributions of the square of the missing mass for events fitting the $K_1^0 K_1^0 n$ hypothesis with χ^2 probabilities greater than 1% for a subsample of the data. The procedure for estimating the contamination due to $K_1^0 K_1^0 n \pi^0$ events is described in the text. The shaded events in the figure represent the estimated contamination.

¹⁸ K. W. Lai (private communication); see also Ref. 5.

FIG. 7. Dalitz plots for the final data sample. Each event is plotted twice, corresponding to the two $K_1^0 n$ mass combinations.



IV. DATA

A. Uncorrected Data

The Dalitz plots for the reaction $\pi^- p \rightarrow K_1^0 K_1^0 n$ at 4 and 5 GeV/c are shown in Fig. 7. Each event is plotted twice, corresponding to the combination of each of the two K_1^0 mesons with the neutron. The existence of structure in the $K_1^0 K_1^0$ system, particularly just above threshold, is evident.

The presence of structure can be seen more clearly in the projections on the mass axes. Figure 8 shows the distributions of $K_1^0 n$ effective mass (each event plotted twice), together with the shapes of the nonresonant

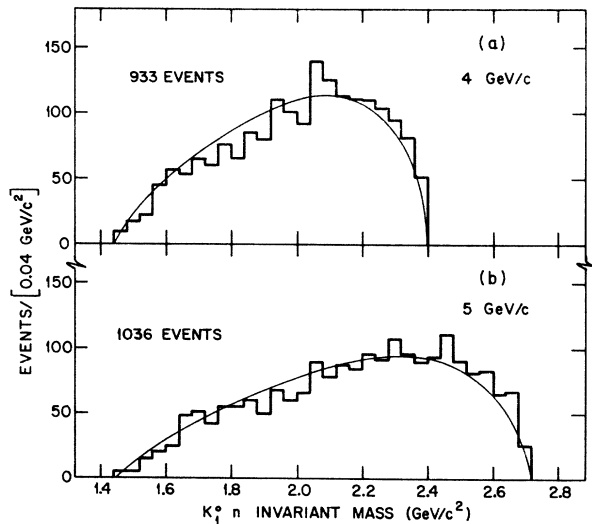


FIG. 8. Distributions of the $K_1^0 n$ invariant mass for events in the final data sample. Each event is plotted twice, corresponding to the two $K_1^0 n$ mass combinations.

distributions as obtained from a Monte Carlo study discussed below. Since the $K_1^0 n$ distributions are consistent with the nonresonant distributions, we conclude that $Y_0^*(1520)$ production is small at 4 and 5 GeV/c. This result supports similar findings by Crennell *et al.*⁵ at 6 GeV/c and Beusch *et al.*⁶ at 5, 7, and 12 GeV/c. However, Alexander *et al.*² and Dahl *et al.*⁴ have reported $Y_0^*(1520)$ production below 4 GeV/c.

The projections onto the $K_1^0 K_1^0$ mass axis are shown in Fig. 9. The data have been corrected for detection efficiency, in accordance with the results of a Monte Carlo calculation described below. Also shown are the

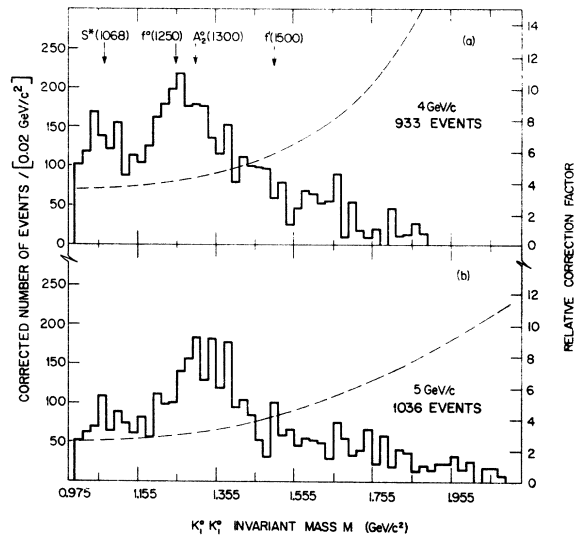


FIG. 9. Corrected distributions of the $K_1^0 K_1^0$ invariant mass corresponding to 933 and 1036 events at 4 and 5 GeV/c, respectively. The dashed curves represent the relative correction factors obtained from Monte Carlo calculations.

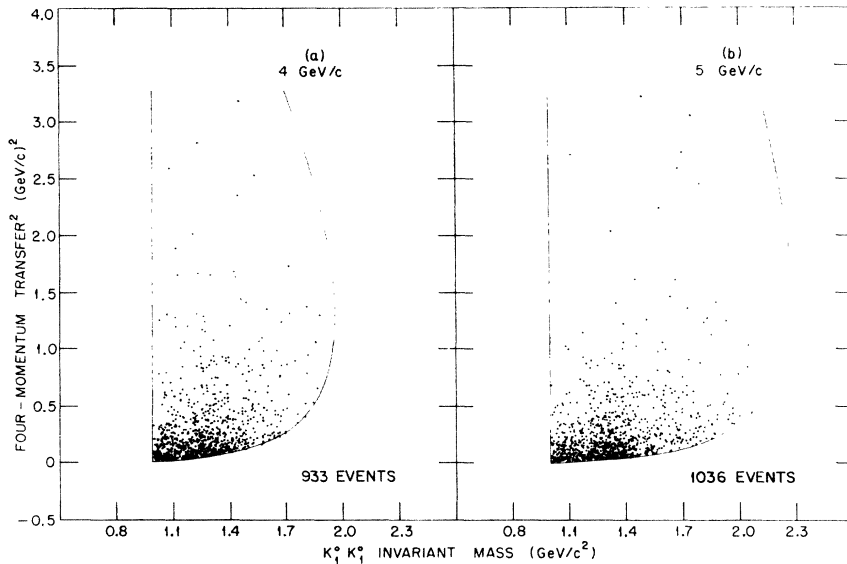


FIG. 10. Chew-Low distributions for the final data sample.

positions of the $f^0(1250)$, $A_2^0(1300)$,¹⁹ and $f'(\sim 1500)$ mesons, each of which is known to be produced in π^-p interactions, and which might be expected to decay via a $K_1^0 K_1^0$ mode. The position of the $S^*(1068)$ “resonance” is also indicated.

The distributions of the square of the four-momentum transfer from target proton to final-state neutron as a function of $K_1^0 K_1^0$ invariant mass are shown in the Chew-Low plots in Fig. 10. The clustering of events at the lowest values of momentum transfer clearly indicates the peripheral nature of K_1^0 -pair production.

B. Correction Factors

A Monte Carlo study was performed to determine the detection efficiency of the magnet-spark-chamber spectrometer, and to investigate the possibilities of biases introduced by the triggering requirement and the system geometry. Events of the reaction $\pi^-p \rightarrow K_1^0 K_1^0 n$ at 4 and 5 GeV/c were generated²⁰ according to phase space weighted by a peripherality factor $e^{\beta t}$, where $-t$ is the square of the four-momentum transfer. The value $\beta=2$ was found to provide an adequate description of the $K_1^0 K_1^0$ mass spectrum, except for

¹⁹ It should be noted that there is a growing body of evidence indicating a split in the A_2 peak, the earliest report being that of B. Levrat, C. A. Tolstrup, P. Schubelin, C. Nef, M. Martin, B. C. Maglič, W. Kienzle, M. N. Focacci, L. Dubal, and D. Chikovani, *Phys. Letters* **22**, 714 (1966). Indeed, a recent work by D. J. Crennell, U. Karshon, K. W. Lai, J. M. Scarr, and I. O. Skillicorn [*Phys. Rev. Letters* **20**, 1318 (1968)] claims evidence for such an effect based on an investigation of the $K_1^0 K_1^0$ mode. Unfortunately, limited resolution prevented further exploration of this interesting possibility. For a review of the present situation, see the discussion on the A_2 contained in *Proceedings of the Informal Meeting on Experimental Meson Spectroscopy, Philadelphia 1968*, edited by C. Baltay and A. H. Rosenfeld (W. A. Benjamin, Inc., New York, 1968).

²⁰ G. R. Lynch, University of California Research Laboratory Report No. UCRL-10335, 1962 (unpublished).

regions where enhancements occurred.²¹ Secondaries from the $K_1^0 \rightarrow \pi^+ \pi^-$ decays were traced through the system, and were tested for compatibility with the triggering and editing requirements.

The effects of these requirements were studied by comparing the distributions of various quantities of interest for the “generated” and “triggering” events. Correction functions were obtained by dividing the generated distributions by the triggering (observed) distributions, bin by bin, and then smoothing the resulting quotient distributions to remove statistical fluctuations.

The resulting correction functions for the $K_1^0 K_1^0$ invariant-mass distributions are shown in Fig. 9. The rising correction function (decreasing detection efficiency) is readily understood in terms of the increasing number of K 's at large angles relative to the incident beam resulting from the increasing energy available for the decay of the $K_1^0 K_1^0$ system and the spectrometer's small acceptance for such events.

A similar procedure was applied to the distribution of four-momentum transfer over the entire $K_1^0 K_1^0$ mass range. The resulting correction functions were found to increase considerably with increasing $|t|$. However, K_1^0 pairs in the low-mass region are produced predominantly in peripheral interactions, and the correction functions at these low values of $|t|$ are essentially flat.

The effects of the triggering and editing requirements on the Gottfried-Jackson (GJ) decay angular distributions²² for the $K_1^0 K_1^0$ system were also investigated. For events generated in accordance with flat distributions in both $\cos\theta_{GJ}$ and ϕ_{GJ} , the distributions

²¹ The results were found to be relatively insensitive to the exact value of the peripherality factor.

²² K. Gottfried and J. D. Jackson, *Nuovo Cimento* **33**, 309 (1964).

for triggering events were found to be flat for low $K_1^0 K_1^0$ invariant masses (below about $1.1 \text{ GeV}/c^2$); at higher masses, however, a strong bias with respect to $\cos\theta_{GJ}$ was observed, the detection efficiency decreasing for events with $|\cos\theta_{GJ}|$ near zero. This decrease in detection efficiency can again be understood in terms of large-angle K 's which become more prevalent with increasing energy of the $K_1^0 K_1^0$ system.

V. RESULTS

A. Corrected Data

The final $K_1^0 K_1^0$ invariant-mass distributions, corrected in accordance with the Monte Carlo calculation described above, are shown in Fig. 9. The average uncertainty in the mass determination is approximately $20 \text{ MeV}/c^2$ up to about $1.2 \text{ GeV}/c^2$, and increases slowly to approximately $40 \text{ MeV}/c^2$ at high masses. Both the 4- and the 5-GeV/c data exhibit an enhancement in the region near threshold, as well as a large, rather broad peak near $1.3 \text{ GeV}/c^2$. This latter peak is attributed to the $K_1^0 K_1^0$ decay mode of the f^0 and A_2^0 mesons, whose individual contributions are not resolved (see Sec. V C). There is no significant indication of the peak near $1.44 \text{ GeV}/c^2$ reported by Beusch *et al.*,⁶ nor is there evidence for the f' (~ 1500) production reported by Crennell *et al.*⁵

B. Threshold Enhancement

Since the threshold enhancement in the $K_1^0 K_1^0$ system was a principal point of interest in this experiment, particular emphasis has been placed on investigating the "threshold region," the region of $K_1^0 K_1^0$ invariant mass less than $1.135 \text{ GeV}/c^2$ shown in Fig. 11. The Monte Carlo correction factor is essentially flat over this mass interval.

Shown in Fig. 12 are the distributions of the square of the four-momentum transfer from target proton to final-state neutron, $-t$, for events in the threshold region. The data are well fitted by the form $e^{\alpha t}$ with α equal to 6.3 ± 0.8 and $6.9 \pm 0.8 \text{ (GeV}/c)^{-2}$ at 4 and

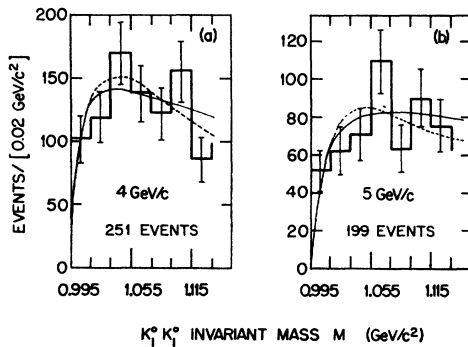


FIG. 11. Corrected distributions of the $K_1^0 K_1^0$ invariant mass for the threshold region. The solid curve represents the results of the scattering-length fit; the dashed curve is a resonance form.

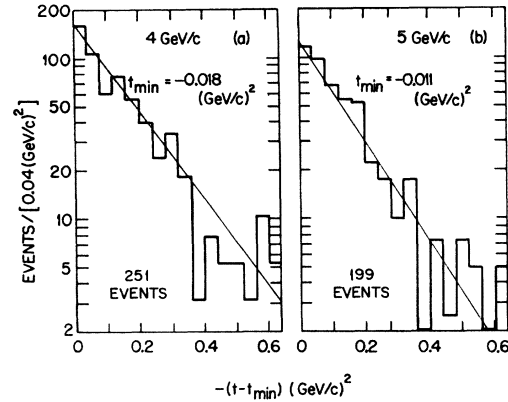


FIG. 12. Corrected distributions of the four-momentum transfer squared from target proton to final-state neutron for events in the threshold region. For convenience the abscissa is plotted in terms of $t-t_{\min}$, where t_{\min} is the kinematic minimum at threshold.

5 GeV/c, respectively, demonstrating again the high degree of peripherality characteristic of these events.

The Gottfried-Jackson angular distributions²² are shown in Fig. 13. Both the $\cos\theta_{GJ}$ and the ϕ_{GJ} distributions are consistent with isotropy, indicating that the dynamics of the threshold enhancement are consistent with one-pion exchange and with an s -wave interaction at the meson vertex shown in Fig. 14. However, as the upper mass limit is raised, a non-isotropic admixture appears, presumably resulting from the presence of the f^0 and A_2^0 mesons.

Two interpretations of the threshold enhancement have been investigated as described below.

1. Scattering-Length Interpretation

Following Alexander *et al.*,² the Chew-Low approach toward the scattering of unstable particles⁸ has been combined with the multichannel reaction-matrix formalism of Dalitz and Tuan,²³ resulting in a description of the threshold enhancement in terms of a complex scattering length. From the results of Chew and Low,⁸ the reaction $\pi N \rightarrow K \bar{K} N$, dominated by one-pion exchange at low values of $-t$, is related to the virtual process $\pi^- \pi^+ \rightarrow K \bar{K}$ occurring at the meson vertex (see Fig. 14) by

$$\frac{d^2\sigma(\pi N \rightarrow K \bar{K} N)}{dM dt} = \frac{f^2}{2\pi} \frac{2M^2 p}{p_{\text{inc}}^2 m_\pi^2 (m_\pi^2 - t)^2} \frac{t}{\sigma(\pi\pi \rightarrow K \bar{K})}$$

Here, M is the invariant mass of the $K \bar{K}$ system, p_{inc} is the momentum of the incoming beam pion, p is the barycentric momentum of a pion in a $\pi\pi$ system of total energy M , m_π is the pion rest mass, and f is the π^0 -nucleon coupling constant. Expressing the interaction in terms of a zero-effective-range, complex-scattering length for the s -wave isoscalar $K \bar{K}$ system,

²² R. H. Dalitz and S. F. Tuan, *Ann. Phys. (N. Y.)* **3**, 307 (1960); R. H. Dalitz, *Strange Particles and Strong Interactions* (Oxford University Press, London, 1962).

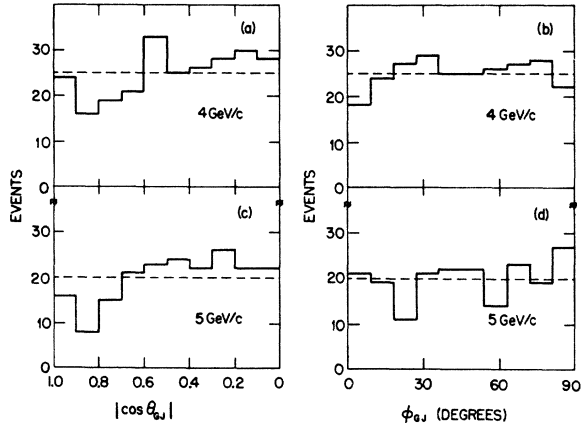


FIG. 13. Gottfried-Jackson angular distributions for events in the threshold region (251 events at 4 GeV/c and 199 events at 5 GeV/c).

the reaction-matrix formalism yields

$$\sigma(\pi\pi \rightarrow K\bar{K}) = 4\pi \frac{q}{p^2} \frac{2b}{(1+bq)^2 + (aq)^2},$$

where $A = a + ib$ is the complex-scattering length and q is the K momentum in the $K\bar{K}$ barycentric system.

Applying these results to the reaction $\pi^- p \rightarrow K_1^0 K_1^0 n$ yields a $K_1^0 K_1^0$ invariant-mass spectrum of the form

$$\frac{dN}{dM} \propto \frac{M^2 q}{p_{\text{inc}}^2 p} \left(\int_{t_{\text{min}}}^{t_{\text{max}}} \frac{t}{(m_\pi^2 - t)^2} F^2(t) dt \right) \times \frac{b}{(1+bq)^2 + (aq)^2}, \quad (1)$$

in which $F(t)$ is a form factor introduced to describe the behavior of the t distribution. In our analysis we have used the phenomenological form $F(t) = (\Lambda^2 - m_\pi^2) / (\Lambda^2 - t)$, which gives a good representation of the data with $\Lambda^2 = 0.165$ (GeV/c²)². An analysis based on Eq. (1) yields only the magnitude of a , while b must necessarily be positive.

A maximum-likelihood procedure was used to obtain the scattering-length parameters a and b by fitting the form of Eq. (1) to the threshold enhancement data. The procedure proved to be rather insensitive to the value of b , although $|a|$ could be determined adequately. The results are seen to be quite similar at both momenta:

$$\begin{aligned} |a| &= 1.18_{-0.44}^{+0.31} \text{ F}, \quad b = 0.58 \pm 0.62 \text{ F} \quad \text{at } 4 \text{ GeV}/c, \\ |a| &= 0.98 \pm 0.28 \text{ F}, \quad b = 0.18_{-0.72}^{+0.58} \text{ F} \quad \text{at } 5 \text{ GeV}/c. \end{aligned}$$

The corresponding fits are indicated by the solid curves in Fig. 11. The effects of a possible background were examined by repeating the scattering-length fits for various momentum-transfer cuts, and the results were found to remain essentially unchanged.

2. Resonance Interpretation

The possibility that the threshold enhancement results from an isoscalar, s -wave $K^0\bar{K}^0$ resonance, the S^* , was investigated by fitting the data with a resonance form. The resonance form used was suggested by Jackson,²⁴ who pointed out that the energy dependence of the resonance width and the existence of other decay modes can seriously affect the shape of broad resonances occurring near threshold. These considerations are particularly important in this situation, where the resonance appears just above the $K^0\bar{K}^0$ threshold and may also decay via a $\pi\pi$ mode,²⁵ a consideration omitted in previous analyses.^{5,6}

The data were fitted with the expression

$$\frac{dN}{dM} = \left(N_1 + N_2 \frac{M}{q} \frac{\Gamma_{K_1^0 K_1^0}(M)}{(M^2 - M_0^2)^2 + M_0^2 \Gamma_{\pi\pi}^2(M)} \right) \frac{dF_3}{dM}, \quad (2)$$

where N_1 and N_2 are constants determining the amounts of resonance and background (assumed to be incoherent and proportional to three-body invariant phase space, dF_3/dM), M is the $K_1^0 K_1^0$ invariant mass, and M_0 is the resonance mass. The total (mass-dependent) width is given by $\Gamma_T(M) = \Gamma_{K\bar{K}}(M) + \Gamma_{\pi\pi}(M)$, where $\Gamma_{K\bar{K}}(M)$ and $\Gamma_{\pi\pi}(M)$ represent the partial widths for decay into the observed $K\bar{K}$ mode and the possible $\pi\pi$ mode, respectively. For s -wave decays, these partial widths have the form $\Gamma_{K\bar{K}}(M) = (q/q_0)\Gamma_{K\bar{K}}^0$ and $\Gamma_{\pi\pi}(M) = (p/p_0)\Gamma_{\pi\pi}^0$, where q is the K momentum in the $K\bar{K}$ barycentric system, p is the barycentric momentum of a pion in a $\pi\pi$ system of total energy M , and q_0 and p_0 are the corresponding quantities for a mass M_0 . The terms $\Gamma_{K\bar{K}}^0$ and $\Gamma_{\pi\pi}^0$ represent the values of the partial widths at resonance. From simple isotopic spin considerations, the partial width for decay into the $K_1^0 K_1^0$ final state is $\Gamma_{K_1^0 K_1^0}(M) = \frac{1}{4}\Gamma_{K\bar{K}}(M)$.

The resonance parameters were obtained by fitting Eq. (2) to the data. The background in the threshold region, including contributions from the f^0 and A_2^0 , was estimated to be about 20% at both 4 and 5 GeV/c. The best values of the parameters proved to be very sensitive to the value of the $\pi\pi$ to $K\bar{K}$ branching ratio, $R = \Gamma_{\pi\pi}^0 / \Gamma_{K\bar{K}}^0$. Unfortunately, the evidence for a $\pi\pi$ enhancement in this mass region is inconclusive,²⁵ although an upper limit of $R \leq 2.5$ has been reported.⁵ Consequently, R

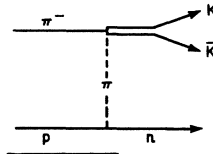


FIG. 14. One-pion-exchange diagram for $\pi^- p \rightarrow K\bar{K}n$.

²⁴ J. D. Jackson, *Nuovo Cimento* 34, 1644 (1964).

²⁵ For a review of the present evidence for a $\pi\pi$ mode, see B. French in *Proceedings of the Fourteenth International Conference on High-Energy Physics, Vienna, 1967* (CERN, Geneva, 1968), p. 101. Also, K. W. Lai in *Proceedings of the Informal Meeting on Experimental Meson Spectroscopy, Philadelphia, 1968*, edited by C. Baltay and A. H. Rosenfeld (W. A. Benjamin, Inc., New York, 1968).

has been treated as a parameter and allowed to vary between 0 and 3.

The dependence of the resonance parameters M_0 and $\Gamma_{\mathcal{T}^0} = \Gamma_{\mathcal{T}}(M_0)$ on R , as determined from the 4-GeV/c data, is shown in Fig. 15. The dashed curves indicate the limiting values (diagonal error terms) obtained by fixing one of the quantities at its best value and varying the other until χ^2 had increased by unity; however, the errors are also highly correlated. Although the effect of R on the parametrization is obviously very important, the shapes of the resonance curves are relatively insensitive to the value of R . The typical resonance shape indicated by the dashed curve in Fig. 11(a) corresponds to $R=0$.

At 5 GeV/c the data did not yield well-defined resonance parameters. Here, the shape of the threshold enhancement is such as to produce large uncertainties for the values of M_0 and $\Gamma_{\mathcal{T}^0}$ corresponding to a given value of R . Thus, in the absence of unique fits, the resonance curve shown by the dashed curve in Fig. 11(b) has been calculated using parameters obtained from the 4-GeV/c data with $R=0$. This curve is a reasonable representation of the data, yielding a χ^2 value of 9.7 with six degrees of freedom as compared with a value of 6.4 with four degrees of freedom, which was obtained for the 4-GeV/c fits. For comparison, the χ^2 values for the scattering-length fits were 7.7 and 6.8 for 4 and 5 GeV/c, respectively, each with four degrees of freedom.

C. Higher Mass Resonances

In addition to the threshold enhancement, the $K_1^0 K_1^0$ invariant-mass spectrum shows a broad enhancement

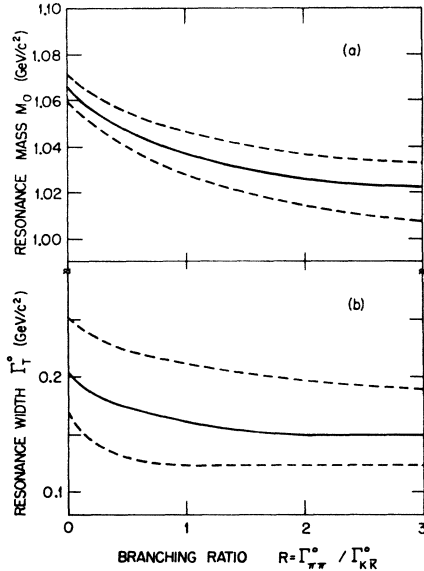


FIG. 15. Resonance parameters as a function of the $\pi\pi$ to $K\bar{K}$ branching ratio for the 4-GeV/c data. The dashed curves represent the limiting values (diagonal error terms) as determined from $(\chi^2)_{\min} + 1$; in addition, the errors are highly correlated.

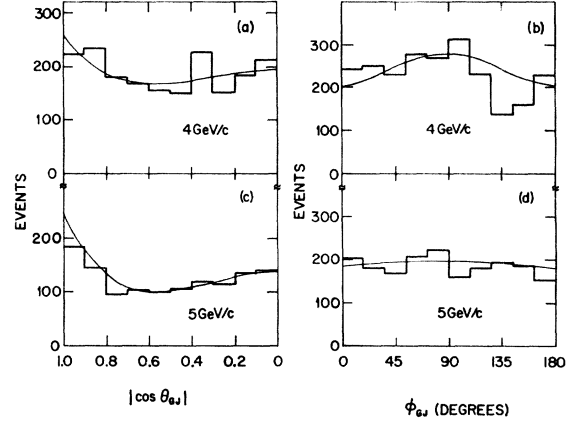


FIG. 16. Gottfried-Jackson angular distributions for the events in the f^0 - A_2^0 region (487 events at 4 GeV/c and 531 events at 5 GeV/c).

centered about 1.3 GeV/c² (see Fig. 9). This structure is attributed to the production of $f^0(1250)$ and $A_2^0(1300)$ mesons. However, attempts to determine the individual f^0 and A_2^0 contributions by fitting the mass spectra were inconclusive. We have also tried to obtain the relative rates for f^0 and A_2^0 production by investigating the Gottfried-Jackson angular distributions²² for events with $K_1^0 K_1^0$ invariant mass in the interval between 1.14 and 1.40 GeV/c².

If f^0 production is dominated by π exchange and A_2^0 production is dominated by ρ exchange, then the angular distributions for the f^0 meson are

$$W_f(\theta_{GJ}, \phi_{GJ}) = \frac{5}{16\pi} |C_1|^2 (3 \cos^2 \theta_{GJ} - 1)^2$$

and, for the A_2^0 meson,

$$W_{A_2}(\theta_{GJ}, \phi_{GJ}) = (15/8\pi) |C_2|^2 \sin^2 \theta_{GJ} \times \cos^2 \theta_{GJ} (1 - \cos 2\phi_{GJ}).$$

The constants $|C_1|^2$ and $|C_2|^2$ are the intensities for the f^0 and A_2^0 , respectively. Since no interference between the f^0 and A_2^0 amplitudes is possible in this simple model, the total angular distribution was taken to be the incoherent sum of the above two expressions together with an isotropic, noninterfering background.

The 487 events at 4 GeV/c and the 531 events at 5 GeV/c which fall in the $K_1^0 K_1^0$ invariant-mass interval between 1.14 and 1.40 GeV/c² were fitted with this hypothesis using a maximum-likelihood calculation. The raw data were corrected for the dependence of the detection efficiency on $\cos \theta_{GJ}$ and ϕ_{GJ} by using results of the Monte Carlo study described previously. The results of the fitting procedures are shown in Fig. 16. The curves are normalized to the number of corrected events. The fitted values of $|C_1|^2$ and $|C_2|^2$ are

$$\begin{aligned} |C_1|^2 &= 0.11 \pm 0.04, & |C_2|^2 &= 0.04_{-0.02}^{+0.03} & \text{at } 4 \text{ GeV/c,} \\ |C_1|^2 &= 0.24 \pm 0.05, & |C_2|^2 &= 0.00 \pm 0.06 & \text{at } 5 \text{ GeV/c.} \end{aligned}$$

The small values of $|C_2|^2$ imply very little A_2 production, particularly at 5 GeV/c. However, the $K_1^0 K_1^0$ invariant-mass distributions (Fig. 9) clearly indicate that the enhancement in the 1.3-GeV/c² region is too broad to be attributed entirely to f^0 production. Moreover, the distribution in $\cos\theta_{GJ}$ differs from that reported by Eisner *et al.*²⁶ in their study of the $\pi\pi$ decay of the f^0 at 4.16 GeV/c.

A recent analysis by Fischer,²⁷ who also studied the angular distributions for $K_1^0 K_1^0$ decays of f^0 and A_2^0 mesons, indicates that even absorption corrections are insufficient to account for the observed data. Fischer points out that the presence of broad overlapping resonances together with a substantial amount of background give rise to interference effects which complicate the spin configuration of the resonances and which cannot be ignored (as was done here).

VI. CONCLUSIONS

In an attempt to bridge the existing data and thereby clarify certain inconsistencies, we have investigated the reaction $\pi^- p \rightarrow K_1^0 K_1^0 n$ at 4 and 5 GeV/c. At both momenta, the $K_1^0 K_1^0$ invariant-mass distributions clearly indicate the existence of an enhancement just above threshold, as well as a large, rather broad peak near 1.3 GeV/c². This latter peak is attributed to the $K_1^0 K_1^0$ decay mode of the f^0 and A_2^0 mesons. However, neither attempts to fit the mass distributions nor investigations of the angular distributions succeeded in determining the individual f^0 and A_2^0 contributions. No substantial evidence was found for either $G(\sim 1440)$ ⁶ or for $f'(1500)$ ⁵ production. An examination of the $K_1^0 n$ system revealed no evidence for $Y_0^*(1520)$ production.

The threshold enhancement in the $K_1^0 K_1^0$ system has been analyzed from two different viewpoints: (1) as resulting from an isoscalar, s -wave $K^0 \bar{K}^0$ interaction characterizable in terms of a large complex-scattering length, and (2) as arising from an $I=0$, $J^P=0^+$ resonant state. The data obtained in this experiment are equally well described by either of these hypotheses. The analysis in terms of a nonresonant interaction permits the determination of the real part of the scattering length, and the results so obtained are essentially identical at both 4 and 5 GeV/c. When described in terms of a resonance, however, the determination of the resonance parameters was found to be strongly dependent on the value of the $\pi\pi$ to $K\bar{K}$ branching ratio, and this value is currently the subject of considerable dispute.

²⁶ R. L. Eisner, P. B. Johnson, P. R. Klein, R. E. Peters, R. J. Sahni, W. L. Yen, and G. W. Tautfest, *Phys. Rev.* **164**, 1699 (1967).

²⁷ W. E. Fischer, *Helv. Phys. Acta* **40**, 749 (1967); *Nuovo Cimento* **59A**, 29 (1969). The data for this analysis were obtained in the experiment described in Ref. 6.

The results of our scattering-length fits are compatible with the Berkeley values obtained at lower momenta.²⁻⁴ Although the invariant-mass distributions from our experiment are similar to those reported by Beusch *et al.*⁶ at 5, 7, and 12 GeV/c, these authors could not obtain satisfactory scattering-length fits, and interpreted their threshold enhancement as a scalar meson with parameters $M_0 = 1.079_{-0.005}^{+0.006}$ GeV/c² and $\Gamma_0 = 0.168_{-0.019}^{+0.021}$ GeV/c²; the effect of a possible $\pi\pi$ mode on the parametrization was not considered. On the other hand, the data from our experiment appear substantially different from those obtained by Crennell *et al.*⁵ at 6 GeV/c², in which a comparatively narrow peak well above threshold was observed, and which was interpreted as a scalar meson with parameters²⁸ $M_0 = 1.068 \pm 0.010$ GeV/c² and $\Gamma_0 = 0.080 \pm 0.015$ GeV/c².

In summary, it now seems that the existence of the S^* resonance cannot be established solely by more precise investigations of the $K\bar{K}$ system, in view of the threshold and multichannel complications discussed above. Information about the $\pi\pi$ system, particularly the $\pi^0\pi^0$ state (which cannot be formed from ρ decay) is needed. Finally, there remains the possibility that this enhancement is due to *both* a large s -wave scattering length and a scalar resonance.²⁹

ACKNOWLEDGMENTS

We are grateful for the assistance and cooperation of the ZGS personnel at the Argonne National Laboratory. We wish to acknowledge the indispensable assistance of W. Evans, D. Jankowski, G. Niemeyer, and W. Rickhoff, as well as the major contributions of the scanning and measuring staffs at the three institutions. We are also grateful for assistance rendered by personnel of the ANL and Notre Dame computer centers. One of us (TFH) wishes to thank Professor R. Hildebrand for encouragement and support during the construction of the spectrometer and acknowledges valuable conversations with Professor I. Pless regarding hydrogen-target design. Another of us (THG) acknowledges support received from Purdue University during the initial year of the experiment. The U.I.C.C. authors (SB, SM, DWMcL) wish to acknowledge support received from the University Research Board, and to thank the Argonne National Laboratory for Visiting Scientist appointments.

²⁸ These data were fitted using a Breit-Wigner form having a constant width, and no provision was made for a possible $\pi\pi$ decay mode. However, because the enhancement is narrow and almost a full width above threshold, these factors have little or no effect on the parametrization. This is not the case for our data nor for the data of Ref. 6.

²⁹ G. Goldhaber, in *Proceedings of the Thirteenth International Conference on High-Energy Physics, Berkeley, 1966* (University of California Press, Berkeley, 1967), Session 7, p. 103.